Analysis of particle rearrangements during sintering by microfocus computer tomography (µCT)

M. Nöthe, M. Schulze, B. Kieback, H.-G. Maas

Technische Universität Dresden, Institute of Materials Science, Helmholtzstr. 7, 01060 Dresden, Germany

Abstract

The theoretical description of sintering processes based on two particle models shows a significant discrepancy of the predicted and observed shrinkage of real powder specimens. This inconsistence is caused by particle rearrangement processes as observed in particle rows, 2D specimens and on the surface of 3D samples. Only the application of microfocus computer tomography (µCT) combined with photogrammetric image analysing gives the opportunity to determine particle rearrangements inside of 3D specimens.
The analysis of the particle rearrangements during successive sintering stages is shown. Samples consisting of 100…120 µm copper balls were sintered. The sintering was interrupted frequently to enable the acquisition of 3D datasets of successive sintering stages by µCT. Photogrammetric image analysing was used to determine the particle positions, the particle contacts for each dataset. In addition each particle was tracked from the initial sintering stage to the final sintering stage. The particle rotation, the formation and breaking of contacts are presented. The article shows a detailed statistical analysis of the correlations between these parameters. Especially the contribution of particle rotations to the sintering process is analyzed in detail.

Introduction

The theoretical description of sintering processes is usually founded on the assumption, that the surface free energy is the main driving force of sintering. In this model the growth of interparticle contacts is accompanied by material transport from the contact zone to the surface. The material transport leads to the particle centre approach [1,2,3]. If no additional particle rearrangements occur this model is suitable to determine the shrinkage of a specimen [4]. Unfortunately in real specimens with complex geometries shrinkage rates inconsistent with this prediction occur. The discrepancy is to be attributed to cooperative material transport processes, e.g. particle rearrangements by rotation [1,5,6]. Possible driving forces are:

- the desire to form low energy grain boundaries in the particle contacts [7],
- tensions caused by asymmetric sintering contact zones and
- tensions caused by inhomogeneous particle centre approach due to inhomogeneous packing of particles with differing particle sizes

Model experiments using rows of particles, 2D arrangements of particles or the observation of the surface of 3D specimens proved that cooperative material transport mechanisms can significantly contribute to the shrinkage of specimens. Microfocus computer tomography (µCT) is the first method with the capability to prove such processes inside of 3D samples [8,9] and can provide data necessary to improve existing computer simulations of sintering (e.g. [10,11]).

Experiments

Spherical copper powder (ECKA Granulate AK 0.1 – 0.125 mm) was sieved to obtain 100..120 µm copper particles. The separation of non spherical particles was performed by rolling over a slightly inclined glass plate. The spherical fraction was filled into crucibles (Ø 2.5 mm). The number of particles obtained by 3D image analysis was 9000…10,000 particles. The crucibles were marked by 6 cuts to determine the orientation of the samples in each 3D image and to measure the precise voxel size. To fix the particles in their positions the specimens were pre-sintered at 600 or 1050 °C in a hydrogen atmosphere. These initial states of the samples were analyzed by µCT (figure 1). The tube voltage was set to 175 KV and the radiation was filtered by a 0.8 mm copper filter to optimize the image quality. The CCD camera resolution was set to 1024*1024 pixels and 1440 projections were acquired. Details on the additional performed beam hardening correction are given in [8]. Then the next sintering stage was prepared by heating the specimen to the sintering temperature, holding the temperature for a defined time (0 min. in case of a temperature series – specimen 1 - with sintering temperatures of 700, 800, 900, 1000 and 1050 °C or 5, 10, 20, 40, 80 and 160 min. in case of a time series sintered at 1050 °C, referred as specimen 2) and freezing the state of sintering for the next µCT analysis by rapidly cooling the sample to room temperature. The images were matched using the notches detected by image analysing as pass points for the 3D least square matching (LSM).

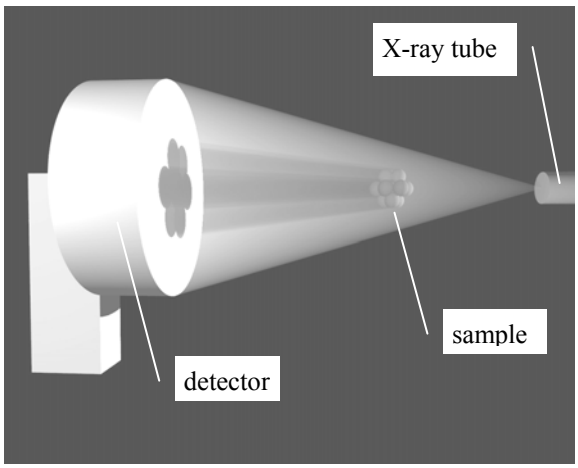

Figure 1 Scheme of the µCT system

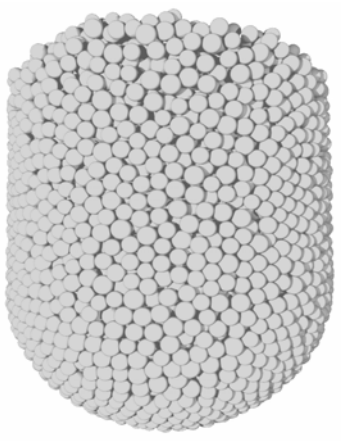

Figure 2 3D image of the initial state of specimen 2

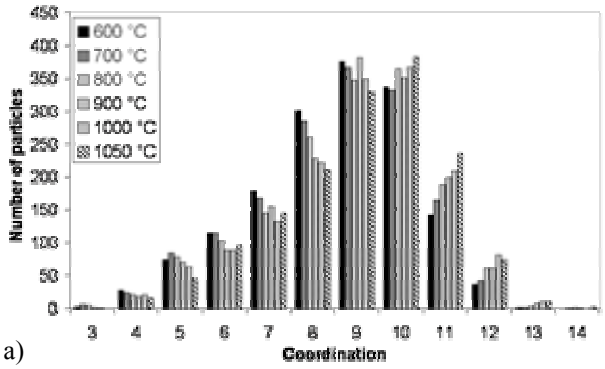

a)

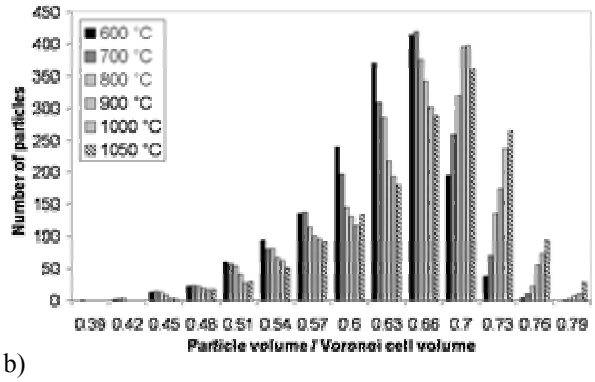

b)

Figure 3 Coordination (a) and density (b) histograms of specimen 1

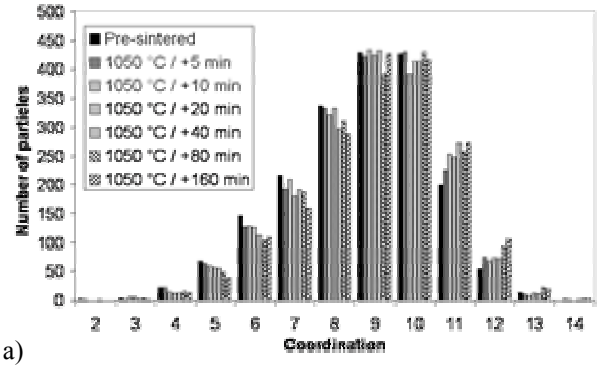

a)

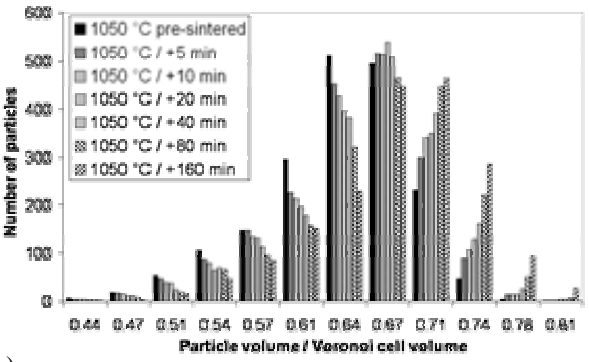

b)

Figure 4 Coordination (a) and density (b) histograms of specimen 2

The particle positions were estimated at first. Then the particle surface points were determined with subvoxel accuracy. An example 3D visualization based on the image analysing data is shown in figure 2. During this step the coordination partners were determined as well. By least squares method a sphere function was fitted to the surface points to determine the particle centre with an error of about 0.1 voxels. Some particles (30...40) were unsuitable (hollow particles) for the used image analysis algorithms. Thus we take into account that 0.5% or less of the particles were not detected or not tracked or the particle centre position was determined with a large error. A reduction of the anyway marginal contribution of erroneous centre positions was performed by excluding rotations larger than the mean rotation plus 5 times the standard deviation.

To calculate the rotation associated to a particle all particles that were in contact before and after the sintering step as well were determined. The rotation is the average of the absolute changes of angles in all particle triplets consisting of the particle and all possible pairs of coordination partners. The number of new and broken inter particle contacts was a by-product of this analysis. Additional parameters were the distance to the next coordination partner and the volume of the Voronoii cell associated to the particle in relation to the particle volume.

The densities of the parameters were assigned to each particle as follows. All particles inside a sphere with a radius of 4 particle diameters around the respective particle were determined (we estimate from the local density of the specimens that each data point represents an average of about 170 values). The densities of the

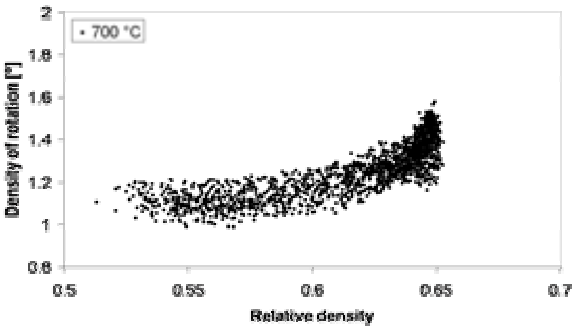

Figure 5 Density of rotation during the 1st sintering step vs. local density of the pre-sintered sample 1

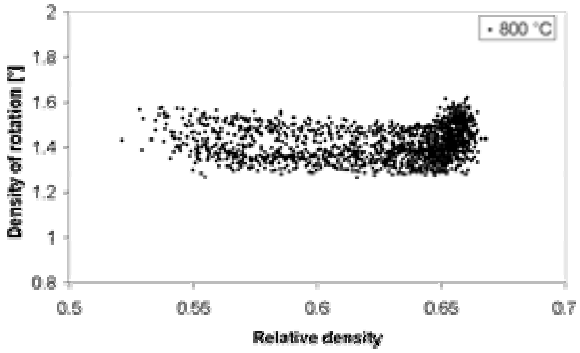

Figure 6 Density of rotation from initial to 2nd sintering step vs. initial local density

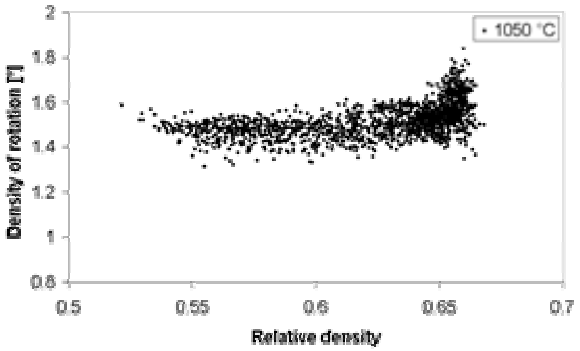

Figure 7 Density of rotation from initial to final sintering step vs. initial local density

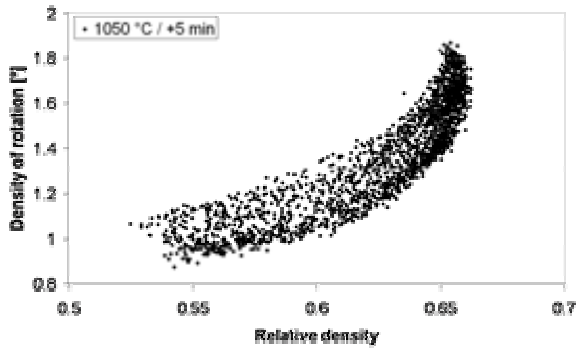

Figure 8 Density of rotation during the 1st sintering step vs. local density of the pre-sintered sample 2

parameters were calculated as the average of the parameter values of all particles in the sphere. In case of the local densities the average was weighted with the volumes of the particles..
Only particles with a distance of more than 4 average particle diameters to the next edge particle were included in the statistical analysis.

Results

Figure 3 a shows the coordination histograms of the specimen sintered at incrementally increased temperatures. The most frequent coordination numbers are 9 and 10 through all stages of sintering and in all specimens (the average coordination is 8.5 to 9). During the process of sintering the number of particles with a coordination of 9 or less decreases and the number of particles with higher coordination increases simultaneously. This indicates an increase of density as shown in figure 3 b. The additional statistical evaluation of broken and new inter particle contacts proved, that in all stages of sintering 300…450 contacts broke up and 450...650 new contacts were formed. Thus a particle rearrangement must take place. The specimen sintered at 1050 °C with increasing holding times showed a similar behaviour as plotted in figures 4 a and b.
Figure 5 shows the densities of particle rotations measured in sample 1 after the first stage of sintering plotted versus the local density of the pre-sintered specimen. The determined densities of rotation have a value of about 1.1 ° in areas with local densities below 60% of full density. With increasing local density the error of measurement exceeds the particle rotation (for the typical relations of error of angle measurement with respect to the local density please refer to figure 8). As the rotations measured during a single sintering step were close or below the margin of error, the analysis of sintering was performed by measuring the total rotation from the initial state of the specimens to the respective stage of sintering. Specimen 1 shows an accumulated rotation of about 1.5 ° from the initial stage of sintering to the 2nd stage of sintering plotted vs. the local density of the pre-sintered specimen. The rotation slightly decreases with increasing local density and merges with the error of angle measurement for densities above 65 %. The accumulated rotations measured for the subsequent stage of sintering show no significant changes. Figure 7 shows the rotation densities accumulated during the entire sintering process vs. the local density of the pre-sintered specimen.
The driving forces for particle rotations are the mismatches of grain boundaries of inter particle contacts. The speed of rotations is expected to decrease after the optimal grain boundary configuration is formed as previously observed using very coarse powders [12,13]. This is consistent with a rotation density slightly above or at least comparable to the error of measurement associated with low local densities during the first sintering step. In addition it has to be concluded, that the most extensive rotation took part during the pre-sintering prior to the first µCT analysis. This conclusion is backed by an extensive swelling observed during pre-sintering of

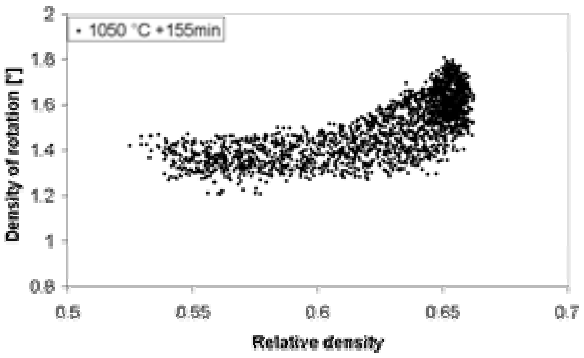

Figure 9 Accumulated density of rotation after the 5th sintering step vs. initial local density

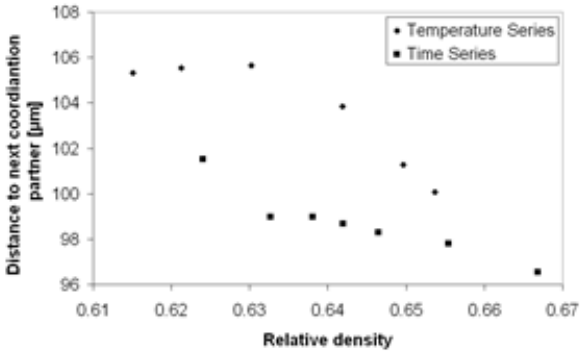

Figure 10 Distance to the next coordination partner vs. local density

specimen for preliminary dilatometer measurements. The accumulated density of rotation measured for subsequent stages of sintering reaches a saturation value after the 2nd stage of sintering. Thus the driving force for particle rotation seems to be almost totally exhausted during the pre-sintering and the first 2 stages of sintering. The counteracting inhibiting force for rotations is the necessity to push away particles in the optimal path of rotation. Thus the insignificant, but for two consecutive sintering steps detected increase of cumulated rotations with decreasing local density is plausible. The saturation of rotations in regions with higher local densities is reached in the final stages of sintering.

Figure 8 shows the densities of particle rotation measured in specimen 2 after the first stage of sintering plotted versus the sample density as representative image of the relation of error of image analysis with the local density. In the following stages of sintering the density of measured accumulated rotation increases and reaches values higher than the error of measurement as shown in figure 9. The accumulated density of rotation still increases during the subsequent stages of sintering.

To assess the contribution of particle centre approach to the densification the mean distances to the next neighbours are plotted in figure 10 versus the local density. The temperature series specimen shows no particle centre approach before the 3rd stage of sintering (900 °C). Thus it can be concluded, that a significant shrinkage due to inter particle neck growth occurs at temperatures of 900 °C or higher. Processes occurring at lower temperatures have to be attributed to particle rearrangements entirely. The second specimen shows a particle centre approach throughout the sintering process.

Conclusion

Specimens consisting of 100...120 µm copper spheres were analysed by microfocus computer tomography. It was possible to measure the coordination of the individual particles. Based on the increasing coordination of the particles and the separately measured density we could prove a densification of the specimens.

We observed the rotations of the particles by measuring the changes of angles in sets of three particles. The largest rotations occurred in the first stages of sintering of the temperature series. In case of the time series the data are interpreted as slow but continuous particle rearrangement.

Acknowledgements

The authors would like to thank the DFG for the funding of our research. Furthermore we are grateful to the ECKA Granulate GmbH & Co. KG for the supply of copper powder.

References

[1] Geguzin, J.E.: Physik des Sinterns, VEB Deutscher Verlag für Grundstoffindustrie, Leipzig, 1973
[2] Schatt, W.: Sintervorgänge, VDI-Verlag 1992
[3] German, R.M., Sintering in theory and practice, John Wiley & Sons, Inc. 1996
[4] Exner, H.E. Jahrbuch „Technische Keramik“, Essen (1988), Vulkan-Verlag, 28
[5] Exner, H.E.; Grundlagen von Sintervorgängen. Berlin/Stuttgart: Gebrüder Borntraeger 1978
[6] Wieters, K.P.: Korngrenzeneinfluß beim defektaktivierten Sintern; Dissertation B; TU Dresden 1989
[7] Sutton, A.P., R.W. Balluffi, Interfaces in crystalline materials, Oxford University press (2003)
[8] Nöthe, M., Pischang, K., Ponížil, P., Bernhardt, R., Kieback, B.: Advances in Powder Metallurgy & Particulate Materials - 2002, ISBN: 1-878954-90-3, Part 13, pp.176-184
[9] Lame O., D. Bellet, M. Di Michiel, D. Bouvard, Nucl. Inst. And Meth. in Phys. Res. B 200 (2003) 287 294
[10] Redanz, P. and R.M. McMeeking, Philosophical Magazine, Vol. 83, p. 2693 (2003).
[11] Olevsky, E.A., Theory of sintering: from discrete to continuum, Mater. Sci. Eng. R23(1998), pp. 41-100
[12] M. Nöthe, K. Pischang, P. Ponizil, B. Kieback. J. Ohser: Investigation of sintering processes by microfocus tomography (µ-CT) in Proc. International Symposium on Computed Tomography and Image Processing for Industrial Radiology 23-25.6.2003 . Berlin, pp. 273-280
[13] M. Nöthe, K. Pischang, P. Ponizil, B. Kieback. J. Ohser: Study of particle rearrangements during sintering by microfocus tomography (µ-CT) in Conference Proceedings EURO PM 2004, 17.10-21.10.2004, Vienna, ISBN 1899072 15 2, Vol.2, pp. 229-234